Interblock and intrablock homogeneity of CAD-CAM composites mechanical properties

Maher ELDAFRAWY[1,2], Yousef KAREVAN[1], Jean-François NGUYEN[3] and Amélie MAINJOT[1,2]

[1] Dental Biomaterials Research Unit (d-BRU), Institute of Dentistry, University of Liège (ULiège), Liège, Belgium
[2] Department of Fixed Prosthodontics, Institute of Dentistry, University of Liège Hospital (CHU), Liège, Belgium
[3] Innovative Dental Materials and Interfaces Research Unit (UR 4462), Université Paris Cité, Montrouge, France
Corresponding author, Amélie MAINJOT; E-mail: a.mainjot@chuliege.be

The purpose of this study was to characterize the homogeneity of the mechanical properties of commercial CAD-CAM composites between different blocks of the same material (interblock homogeneity) and within each block between the internal and external parts (intrablock homogeneity). Tetric CAD (TET); Katana Avencia (KAT); Cerasmart 270 (CER); Grandio (GRN) and Vita Enamic (ENA) were tested for flexural strength (σ_f), flexural modulus (E_f), flexural load energy (U_r) and hardness (HV). Results showed significant differences in interblock homogeneity of σ_f, E_f and U_r for TET, KAT, CER and ENA. In addition, significant differences in interblock homogeneity of HV for TET, CER and GRN were found. Moreover, significant differences in intrablock homogeneity of σ_f, E_f and U_r were found for KAT, CER, GRN and ENA, as well as for HV of all the tested materials except CER. Weibull modulus was highest for GRN, followed by ENA, KAT, TET then CER.

Keywords: Prosthetic dentistry/Prosthodontics, Indirect composites, Polymer-infiltrated ceramic network, Mechanical properties, Flexural strength

INTRODUCTION

CAD-CAM processes have improved the reproducibility of dental prostheses manufacturing and have allowed for the development and use of high-performance materials. Among those materials, CAD-CAM composites are particularly adapted to milling processes since they show better machinability than ceramics, with a higher damage tolerance, faster milling rate and increased bur lifetime[1,2]. They also have a higher edge chipping resistance than ceramics, thus offering smoother margins[3-5], and can be milled in very low thickness, which promote minimally-invasive treatments such as for worn dentition[6,7]. CAD-CAM composites are also particularly adapted to chairside processes since they reduce the manufacturing process time in comparison to some glass-ceramics or zirconia materials, thanks to the absence of additional firing procedures[8]. Furthermore, they can be easily adjusted and repaired by adding direct composite if required[9].

Recently, more and more CAD-CAM composite materials are being launched into the market by manufacturers, especially in the past decade. CAD-CAM composites can be subdivided into two families according to their microstructure: dispersed fillers (DF) and polymer-infiltrated ceramic network materials (PICN)[8]. In DF, the inorganic fillers are randomly dispersed in the organic matrix and polymerized under high-temperature (HT) (>100°C), while PICNs are comprised of a pre-sintered glass-ceramic scaffold that is infiltrated with monomers and polymerized under HT and high-pressure (HP) (180°C - 300 MPa)[10]. Vita Enamic (Vita Zahnfabrik, Bad Säckingen, Germany) is the only marketed PICN, while DF composites are marketed under different commercial names, differing in the composition of the fillers and the organic matrix. Inorganic fillers can vary in their size, weight% and their chemical compositions, for example, zirconia or barium glass fillers, while the organic matrix can also vary in monomer composition and weight% from one material to another[8]. The first-generation of CAD-CAM composites was introduced nearly a decade ago and later on, a second-generation with enhanced mechanical properties was introduced.

In comparison with light-cured direct composites, the HT polymerization of CAD-CAM composites, which is sometimes accompanied by HP, is more homogeneous, less operator dependent and induces less internal stress[11]. Moreover, it results in a higher degree of conversion, reaching up to 96% for experimental PICN[12,13], in comparison to (40–75)% for direct composites[14,15], with a higher degree of crosslinking[11], reflecting on their mechanical properties[16]. Indeed, CAD-CAM composites have higher stiffness and hardness than direct composites, showing higher resistance to wear from opposing teeth[17-19]. The higher degree of conversion also reflects on their chemical stability and water and fluid absorption[15,20]. Additionally, it reduces the amount of unreacted monomers which tend to leach out[15,20] and could lead to toxicity[21,22]. Finally, the industrial process of fabrication of CAD-CAM composites is supposed to result in more homogenous materials with less flaws, notably in comparison with hand-built restorations, therefore improving their mechanical properties[23]. Yet, block manufacturing processes still exhibits some limitations and can engender a certain degree of material inhomogeneity due, for example, to the presence of voids from mixing[24], or polymerization

Received Apr 26, 2023: Accepted Jun 29, 2023
doi:10.4012/dmj.2023-090 JOI JST.JSTAGE/dmj/2023-090

stresses. Unfortunately, manufacturers do not disclose the details about their production procedures.

On the other hand, mechanical characterization of dental restoratives is being carried out before launching the products into the market. Among the tests used for mechanical characterization are hardness and flexural strength, which are simple and standardized methods, most often used by manufacturers and researchers[25]. However, reported data always take into account the average properties of the blocks tested, without mentioning where the sample comes from in the block[26-32]. Ilie[33] studied the intrablock homogeneity of the micromechanical properties of five commercial composite CAD-CAM blocks by evaluating their microhardness indentation through a series of longitudinal and transverse sections cut within each of the blocks. Differences in the micromechanical properties of the analyzed blocks were found between the center and the periphery, rendering them non-homogenous[33]. To the authors' knowledge, there exist no other studies on the homogeneity of the mechanical properties of composite CAD-CAM blocks.

Consequently, the objectives of this study were to characterize the homogeneity of the mechanical properties (flexural strength, flexural modulus, flexural load energy and hardness) of different commercial CAD-CAM composites, including second-generation DF composites and a PICN, between different blocks of the same material (interblock homogeneity) and within each block between the internal and external parts (intrablock homogeneity). The null hypothesis was that, for a same CAD-CAM composite material, there are no interblock or intrablock variations in mechanical properties.

MATERIALS AND METHODS

Five commercially available CAD-CAM composite materials were selected for this study. For each of the composite CAD-CAM materials evaluated, 10 CAD-CAM blocks were tested. Their compositions and lot numbers are displayed in Table 1. Different lot numbers were used to provide close approximation to clinical situations. Indeed, technicians and dentists order blocks at different time intervals and the homogeneity of CAD-CAM composite blocks properties should not be affected by lot number.

Preparation of samples

The supplied CAD-CAM blocks (10 blocks/material) were cut using a low-speed saw (Isomet, Buehler, Lake Bluff, IL, USA) under continuous water irrigation to form 5 rectangular-shaped layers, in which each of the 5 layers was further cut to produce 1.6×4.0×17±0.1 mm bars (3 bars per layer) as shown in Fig. 1 and in accordance with ISO-6872-2015[34] to obtain 15 bars per block (n=150 bars/material and so N=750 bars in total). Bars were polished following ISO-6872-2015[34] recommendations to 20 μm with a diamond pad at 150 rpm under running water (Struers, Ballerup, Denmark). Bars obtained from the middle zone of layers 2, 3 and 4 (Fig. 1), were considered as internal parts of the blocks, in which each block consisted of 3 bars from the internal part and 12 bars from the external part (for intrablock homogeneity). All specimens were tested immediately after preparation, at room temperature.

Table 1 CAD-CAM blocks used in the study and their compositions

Material	Composition		Manufacturer	Lot
	Organic matrix	Inorganic fillers		
Tetric CAD (TET)	Bis-GMA+Bis-EMA+TEGDMA+UDMA	Barium glass (<1 μm)+SiO_2 (<20 nm) (71 wt%)	Ivoclar Vivadent (Schaan, Liechtenstein)	X42815 Z01BGV ZOZOKK ZO2Y4W
Katana Avencia (KAT)	UDMA+TEGDMA	Al_2O_3 (20 nm)+SiO_2 (40 nm) (62 wt%)	Kuraray Noritake (Tokyo, Japan)	L000473 L000484
Grandio Voco (GRN)	UDMA+other DMA	Nanohybrid fillers (87 wt%) Size of fillers unknown	Voco, (Cuxhaven Germany)	2145165 2212243
Cerasmart 270 (CER)	Bis-MEPP+UDMA+DMA	Barium glass (300 nm)+silica (20 nm) (71wt%)	GC (Tokyo, Japan)	1908206 2103011
Vita Enamic (ENA)	UDMA+TEGDMA	Glass-ceramic sintered network (86 wt%, 75 vol%)	Vita Zahnfabrik (Bad Sackingen, Germany)	65900 77100 65971

Data were completed according to manufacturers' information. SiO_2, Silicon oxide; Al_2O_3, Aluminium oxide; Bis-GMA, bisphenol A-glycidyl methacrylate; Bis-EMA, Ethoxylated bisphenol A dimethacrylate; UDMA, urethane dimethacrylate; TEGDMA, triethyleneglycol dimethacrylate; DMA, dimethacrylate; Bis-MEPP, 2,2-Bis(4-methacryloxypolyethoxyphenyl) propane.

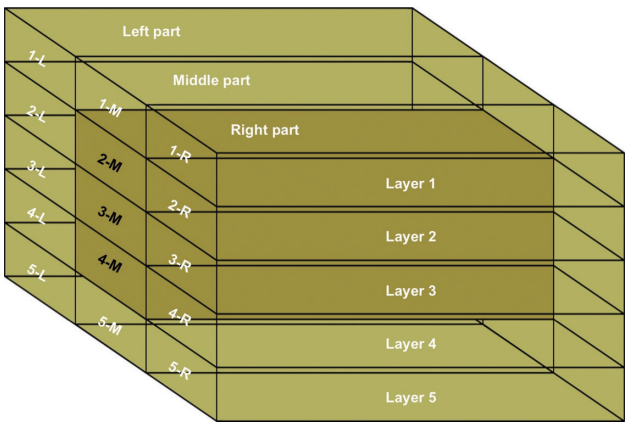

Fig. 1 Schematic representation of a CAD-CAM block cut into 15 bars.
The internal parts are represented by the middle bars of layers 2, 3 and 4 and highlighted in a darker color than the bars of the rest of the block (n=3 bars: 2-M, 3-M and 4-M). The external layers are represented by the rest of the block (n=12 bars). The final dimensions of the bars are 1.6×4.0×17±0.1 mm (total n=15 bars/block). L is the left, M is the middle and R is the right part of the block, while the numbers correspond to the layers.

3-point flexural strength test

Bars were tested in a 3-point bending device (15 mm span width), on a computer-controlled (Bluehill, Instron Canada, Burlington, Canada) universal testing machine (Instron model 5565, with an extensometer) at a cross-head speed of 1 mm/minute to evaluate the flexural strength, flexural modulus and flexural load energy.

Flexural strength, σ_f, was calculated according to the following formula: $\sigma_f = \frac{3FL}{2hc^2}$, where F is the load at fracture, L the span, h the specimen width, and c the specimen height. The values of h and c were measured immediately prior to testing of each sample using a digital caliper (Mitutoyo, Kawasaki, Japan).

Flexural modulus (modulus of elasticity), E_f, was calculated according to the following formula: $E_f = \frac{FL^3}{4hc^3d}$, where d is the deflection corresponding to load F at a point in the straight-line portion of the trace.

Flexural load energy, U_r, was calculated according to the formula: $U_r = \frac{F\Delta}{2}$, where Δ is the maximum deflection.

Hardness

Following the flexural strength test, samples of the middle zone of layer 3 of each of the tested blocks were further polished with 4000 grit silicon carbide paper and tested for microhardness to evaluate the homogeneity at a microscale level. For each sample, three vertical indentations were performed on the periphery and the same was done near the fracture site for both halves of the fractured bars (n=12 indentations/bar, 6 internal and 6 external) using a 25-N loading and 10 s dwell time with the Vickers indenter (Zwick-Rowell, Haan, Germany) with integrated software (Indentec, Zwick-Rowell) to test the Vicker's hardness values (HV).

Digital microscopy analysis

Randomly selected fractured samples (n=4) of each material were further polished at 10 µm diamond pad and then at 3 µm polishing paper with a diamond suspension (~1 µm) to obtain a smooth surface for the examination of flaws under digital microscopy (VHX-7000, Keyence, Chicago, IL, USA).

Scanning electron microscopy (SEM) characterization

The same samples used for digital microscopy were gold-coated and the surface morphology was then further characterized under a scanning electron microscope (SEM; S-3000N, Hitachi, Tokyo, Japan) for images with high magnification.

Statistical analysis

The results comparing the mechanical properties (σ_f, E_f, U_r, HV) of the materials were analyzed by one-way analysis of variance (ANOVA), followed, if warranted, by Scheffé's multiple mean comparisons (α=0.05), using PASW Statistics 18 (SPSS, Chicago, IL, USA). The results of the interblock homogeneity of the mechanical properties (σ_f, E_f, U_r, HV) for each group of materials were analyzed by one-way ANOVA (α=0.05), and the normality of the distribution of their results was assessed with the Shapiro-Wilks test. Mann-Whitney U test was used to compare the mechanical properties (σ_f, E_f, U_r HV) of the intrablock homogeneity for each block (α=0.05). Weibull statistical parameters were calculated for σ_f using the Weibull statistics option in Excel (Microsoft, Redmond, WA, USA). Power analysis was used to calculate the sample size (n=10) for each group based on the formula: $n = \frac{2s^2(Z_{\alpha/2}-Z_{1-\beta})^2}{\Delta^2}$. A clinical significance of 15% (Δ=15) was chosen. The significance level α was set at 0.05, corresponding to a value $Z_{\alpha/2}$=1.96. The desired power (1−β) was set at 80%, corresponding to a value of $Z_{1-\beta}$=0.84. Using these values and the standard deviation (s)[30,31], a sample size of 10 blocks per group was calculated to be n=10.

RESULTS

Mechanical properties

The results of homogeneity between the blocks of the same material (interblock homogeneity), along with the means±standard deviations of their mechanical properties (σ_f, E_f, U_r, HV), statistical analysis and Weibull modulus are represented in Table 2. The tendency graphs of the mechanical properties (σ_f, E_f, U_r and HV) are represented in Fig. 2. GRN showed the highest σ_f significantly, followed by TET, KAT and CER, while ENA had the lowest σ_f significantly. The highest E_f significantly was shown by ENA, followed by GRN,

Table 2 The mechanical properties and Weibull modulus of the CAD-CAM composite materials tested

	σ_f (MPa)			E_f (GPa)			U_r (mJ)			Hardness (HV)			Weibull
	Mean	External	Internal	Mean	External	Internal	Mean	External	Internal	Mean	External	Internal	[CI (95%)]
TET	211.5*[b] (26.4)	211.8 (19.9)	210.3 (23.1)	11.3*[c] (1.3)	11.3 (0.7)	11.3 (0.8)	28.9*[b] (9.3)	28.9 (7.4)	29.0 (8.9)	74.1*[d] (1.6)	73.6 (1.1)	74.6 (1.8)	9.6 [9.3;9.8]
KAT	215.3*[b] (25.4)	216.6 (23.0)	209.9 (19.7)	9.2*[d] (0.6)	9.2 (0.5)	9.2 (0.5)	38.5*[a] (11.3)	39.4 (10.0)	35.2 (8.3)	70.1[d] (3.2)	68.4 (1.7)	73.2 (1.9)	9.7 [9.5;10.0]
CER	219.9*[b] (35.9)	222.8 (31.0)	208.0 (24.2)	11.2*[c] (1.0)	11.3 (0.6)	10.8 (0.5)	30.5*[b] (11.1)	31.3 (9.9)	27.7 (8.1)	87.0*[c] (4.0)	87.0 (4.1)	86.9 (3.3)	7.1 [7.0;7.2]
GRN	242.0[a] (24.3)	242.6 (20.7)	239.6 (24.4)	15.8*[b] (1.7)	15.9 (1.5)	15.5 (1.3)	23.2[c] (5.1)	23.1 (4.8)	23.4 (5.4)	125.8*[b] (4.2)	125.8 (3.8)	125.9 (3.7)	11.8 [11.6;11.9]
ENA	129.3*[c] (13.7)	129.8 (13.0)	127.5 (9.6)	30.7*[a] (2.1)	30.8 (1.6)	30.6 (1.1)	2.9*[d] (0.6)	2.9 (0.5)	2.9 (0.4)	221.9[a] (15.9)	227.1 (9.7)	216.2 (9.6)	11.4 [11.2;11.7]

The results are expressed as the means of the 10 blocks, as well as the means of the internal and external parts, and the standard deviations are represented between brackets. The same superscript letters indicate statistically homogeneous subgroups (1-way ANOVA followed by Scheffé's multiple mean comparisons ($p<0.05$).
* indicates a significant difference in homogeneity between the blocks (interblock) of the same material (1-way analysis of variance followed by Scheffé's multiple mean comparisons $p<0.05$).

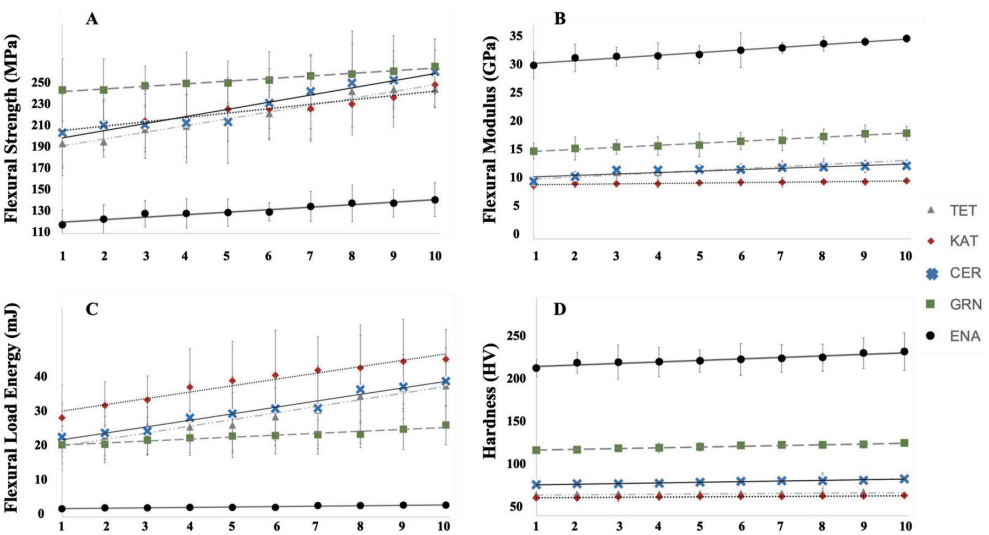

Fig. 2 Tendency curves of the mean and standard deviations.
A, Flexural strength (σ_f); B, Flexural modulus (E_f); C, Flexural load energy (U_r); D, Hardness (HV) of each block of the 10 blocks of the materials tested. Blocks of each material were arranged in ascending order according to their corresponding mechanical properties.

then TET and CER, while KAT showed the lowest E_f significantly. The Value of U_r was significantly highest for KAT, followed by TET and CER, then GRN, while ENA had the lowest U_r significantly. HV were the highest for ENA then GRN, while KAT and TET had the lowest hardness values, significantly. The values of Weibull modulus were highest for GRN, followed by ENA, KAT, TET then CER.

Results of interblock homogeneity showed significant differences ($p<0.05$) between the 10 blocks of the same material in σ_f, E_f and U_r for TET, KAT, CER, and ENA, while GRN showed a significant difference in E_f values but not a significant difference in σ_f and U_r. In addition, significant differences ($p<0.05$) in interblock homogeneity of HV were found for TET, CER and GRN but not for KAT and ENA.

The results comparing the mechanical properties of intrablock homogeneity are represented in Tables 3–6 and their box plots with their medians and interquartile ranges are represented in Fig. 3. Significant differences

Table 3 Mean and standard deviation (between brackets) of the flexural strength (σ_f), and the intrablock homogeneity between the internal and external parts of each of the 10 blocks of the tested materials

Block	TET		KAT		CER		GRN		ENA	
	σ_f (MPa)		σ_f (MPa)		σ_f (MPa)		σ_f (MPa)		σ_f (MPa)	
	Internal	External	Internal	External	Internal	External	Internal	External	Internal	External
1	206.1 (13.1)	205.7 (17.7)	233.4 (42.6)	238.8 (11.1)	234.1 (27.4)	252.7 (15.3)	232.9 (44.2)	240.5 (23.3)	123.7 (5.0)	121.7 (13.6)
2	240.7 (17.5)	232.5 (15.9)	205.3 (5.7)	195.8 (35.6)	243.9 (8.0)	241.5 (28.0)	261.2 (24.8)	243.6 (27.4)	121.1 (22.7)	128.2 (7.7)
3	228.1 (21.3)	233.0 (12.4)	196.8 (13.4)	206.4 (20.1)	216.8 (38.3)	245.2 (46.0)	254.5 (22.6)	253.4 (24.7)	127.7 (5.5)	127.0 (14.0)
4	202.1 (23.0)	216.1 (23.0)	225.1 (16.2)	215.1 (28.0)	220.5 (36.4)	234.8 (32.0)	201.2 (43.5)	241.2 (14.5)	129.3 (9.5)	134.2 (13.7)
5	208.0 (15.6)	197.3 (23.0)	204.4 (13.4)	207.6 (28.0)	219.0 (18.1)	222.7 (32.0)	247.7 (3.4)	250.2 (14.5)	126.9 (6.3)	128.8 (13.7)
6	182.4 (24.3)	190.4 (9.7)	217.5 (19.6)	222.4 (21.1)	191.5 (8.3)	208.6 (37.6)	250.4 (31.5)	240.0 (23.4)	133.6 (19.4)	140.2 (14.0)
7	185.8 (24.9)	187.5 (19.0)	205.6 (11.6)	219.8 (16.7)	221.2 (9.8)	201.9 (39.2)	233.3 (29.2)	240.8 (17.0)	136.8 (5.7)	125.4 (11.9)
8	230.6 (26.5)	215.6 (30.3)	215.7 (8.1)	216.9 (30.5)	163.8 (46.0)	204.9 (31.4)	235.8 (18.5)	237.5 (17.2)	142.4 (9.6)	134.1 (16.9)
9	185.7 (39.3)	206.4 (23.2)	197.3* (36.7)	234.4* (16.3)	189.3 (17.1)	206.6 (22.1)	233.1 (7.7)	248.8 (17.5)	102.8* (4.7)	120.1* (11.8)
10	233.5 (25.8)	233.7 (24.8)	197.6 (30.1)	209.1 (22.2)	179.5 (32.2)	209.5 (26.4)	246.3 (18.6)	230.2 (27.6)	130.8 (7.2)	137.1 (12.5)

* indicates a significant difference in homogeneity within the same block (Mann Whitney *U* test, $p<0.05$).

($p<0.05$) between the internal and external parts were found in σ_f and U_r of KAT block 9, E_f of CER block 1, E_f of GRN block 4 and σ_f and U_r of ENA block 9, higher mechanical properties being found at the external parts of the blocks. HV showed significant differences between the internal and external parts for TET, KAT, GRN and ENA, in which for the DF composites, TET, KAT and GRN, higher HV were found at the center than the periphery, while for ENA it was the opposite. CER showed no statistical difference in HV between the internal and external parts.

Digital microscopy

Images of digital microscopy are shown in Fig. 4. Different kinds of defects can be seen in the selected photos to highlight the possible causes of inhomogeneity within the blocks. While all of the selected samples showed areas of porosities, other samples showed areas of inclusion (Fig. 4A) and areas of higher polymerization shrinkage than the rest of the matrix (Figs. 4B, D).

SEM characterization

SEM images are displayed in Fig. 5. Areas of porosities, areas of higher polymerization shrinkage than the rest of the matrix (Fig. 5A), as well as a large area of inclusion containing voids within (Fig. 5B), were shown at higher magnifications.

DISCUSSION

Significant differences in interblock and intrablock homogeneity of the mechanical properties were detected among the tested groups (Tables 2–6); therefore, the null hypotheses were rejected.

To the authors' knowledge, three studies were performed to evaluate the mechanical properties of GRN[32,35,36], two studies on TET[35,36], and one on KAT[36]. GRN showed σ_f values of 237.4 MPa[32], 264.4 MPa[35] and 266.0 MPa[36] in previous studies, which did not deviate much from the mean obtained in the present study (242.0±24.3 MPa); whereas TET and KAT showed lower mean σ_f in the present study (211.5±26.4 and 215.3±25.4 MPa, respectively) in comparison to literature (229.5 MPa[35] and 254.0 MPa[36] for TET, and 241.0 MPa[36] for KAT) and a reported value of ~230 MPa by the manufacturer of KAT. Meanwhile, more studies

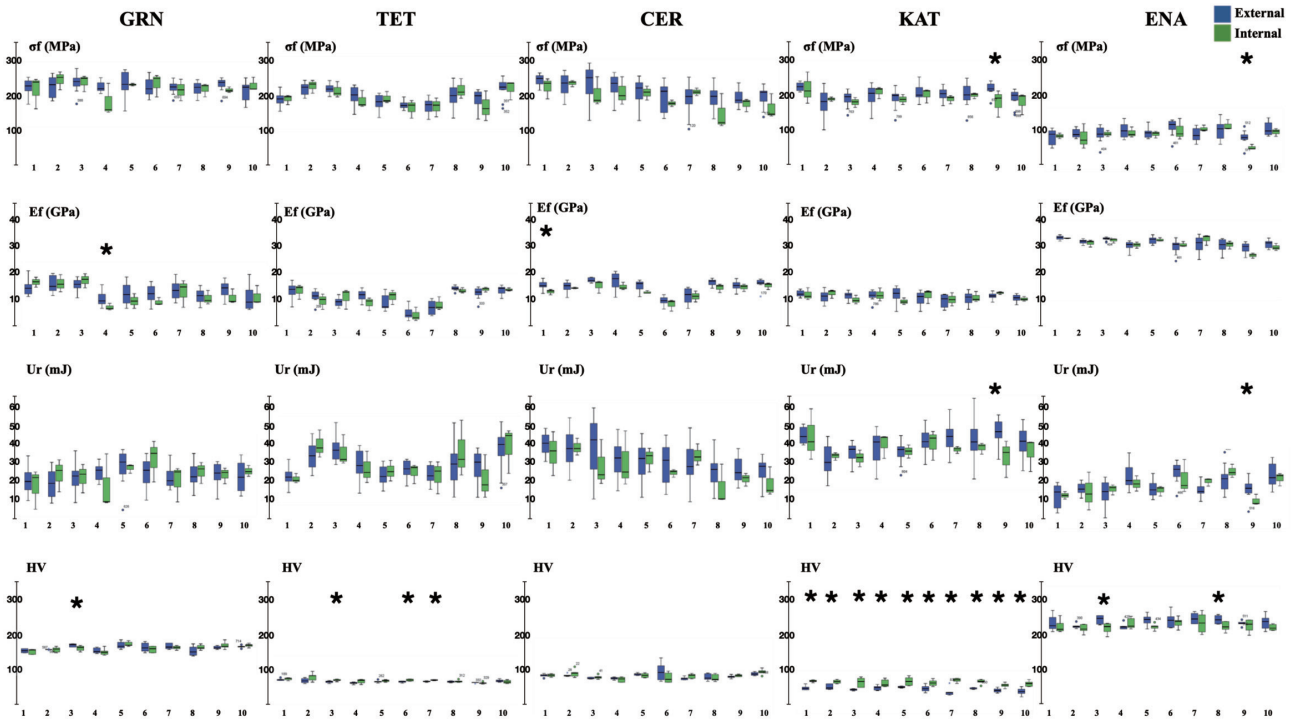

Fig. 3 Box plots showing the median and interquartile ranges and the intrablock homogeneity between the internal and external parts of the five CAD-CAM composites for flexural strength (σ_f); flexural modulus (E_f); flexural load energy (U_r) and hardness (HV).
The Y-axis represents the values of the mechanical properties tested, and the X-axis represents the number of blocks.
* indicates a significant difference in homogeneity within the same block (Mann Whitney *U* test, $p<0.05$).

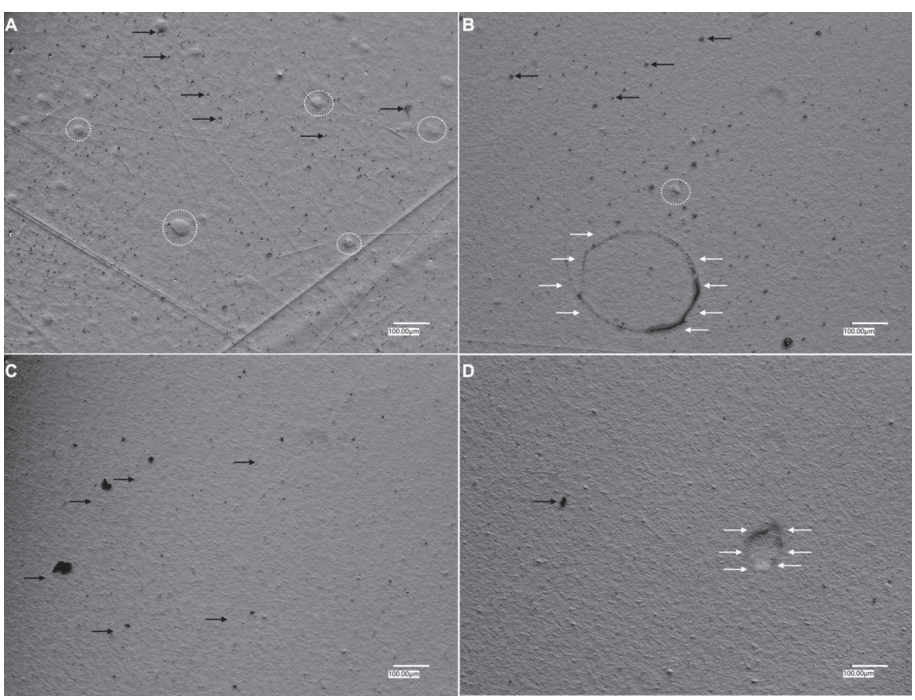

Fig. 4 Digital microscopy images of randomly fractured samples at ×200 magnification showing areas of porosities or voids (black arrows); areas of higher polymerization shrinkage than the rest of the matrix (white arrows) and areas of inclusion (dashed circles).

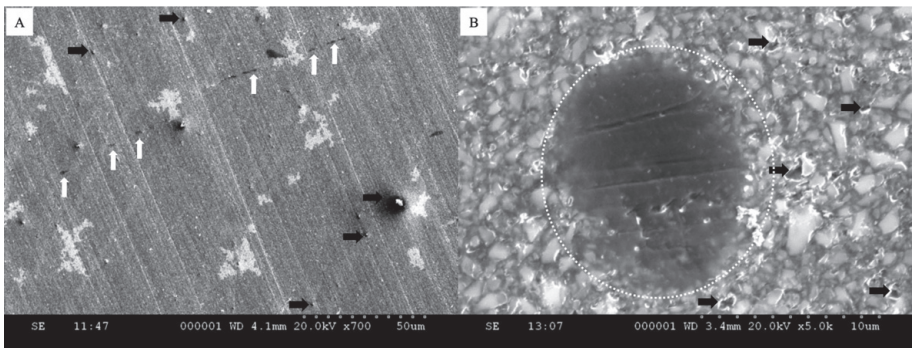

Fig. 5 SEM images showing voids (black arrows), areas of higher polymerization shrinkage than the rest of the matrix (white arrows) and a large area of inclusion containing voids within (dashed circle).
A, 700×; B, 5,000×.

Table 4 Mean and standard deviation (between brackets) of the flexural modulus (E_f), and the intrablock homogeneity between the internal and external parts of each of the 10 blocks of the tested materials

Block	TET		KAT		CER		GRN		ENA	
	E_f (GPa)		E_f (GPa)		E_f (GPa)		E_f (GPa)		E_f (GPa)	
	Internal	External	Internal	External	Internal	External	Internal	External	Internal	External
1	12.3 (1.0)	12.3 (0.9)	9.4 (0.7)	9.5 (0.3)	10.7* (0.3)	11.5* (0.5)	17.6 (0.9)	16.6 (1.2)	32.6 (0.2)	32.8 (0.7)
2	10.9 (1.0)	11.5 (0.7)	9.6 (0.5)	9.2 (0.6)	11.1 (0.1)	11.3 (0.6)	17.4 (1.5)	17.2 (1.4)	30.8 (1.4)	31.4 (0.8)
3	11.4 (1.4)	10.8 (0.6)	8.9 (0.5)	9.3 (0.4)	11.4 (0.8)	12.1 (0.3)	18.0 (1.3)	17.1 (1.1)	31.8 (0.9)	32.4 (0.6)
4	10.6 (0.9)	11.7 (0.7)	9.4 (0.7)	9.3 (0.5)	11.3 (0.5)	12.0 (1.1)	13.2* (0.6)	14.7* (1.3)	30.1 (1.1)	29.8 (1.7)
5	11.5 (0.9)	10.7 (1.0)	8.7 (0.4)	9.4 (0.8)	10.6 (0.2)	11.5 (0.7)	14.3 (1.3)	15.6 (2.0)	32.0 (0.7)	31.9 (1.3)
6	9.1 (0.9)	9.3 (0.8)	9.3 (0.8)	9.0 (0.7)	9.1 (0.7)	9.5 (0.5)	14.1 (0.7)	15.5 (1.5)	30.2 (1.0)	29.5 (2.5)
7	10.5 (0.9)	10.0 (0.9)	8.9 (0.7)	8.7 (0.7)	10.1 (0.7)	10.2 (0.9)	15.9 (2.5)	16.2 (1.5)	32.3 (2.0)	30.5 (3.0)
8	12.3 (0.4)	12.6 (0.3)	9.1 (0.6)	9.0 (0.7)	11.2 (0.5)	11.9 (0.4)	14.8 (1.2)	15.1 (1.2)	30.2 (1.5)	29.9 (2.3)
9	12.4 (0.3)	12.0 (0.7)	9.6 (0.1)	9.3 (0.3)	11.2 (0.5)	11.4 (0.5)	14.9 (1.3)	16.3 (1.3)	26.1 (1.0)	29.0 (2.0)
10	12.4 (0.2)	12.4 (0.5)	8.9 (0.2)	9.0 (0.4)	11.4 (0.4)	11.7 (0.6)	15.0 (1.7)	14.8 (2.0)	29.2 (1.3)	30.4 (1.4)

* indicates a significant difference in homogeneity within the same block (Mann Whitney *U* test, $p<0.05$).

were conducted on ENA[26-28,30,37-40], which showed σ_f in literature ranging between 124.0–202.1 MPa and a reported value of 150–160 MPa by the manufacturer in comparison to this study (129.3±13.7 MPa).

Regarding E_f, in this study, GRN showed a mean value of 15.8±1.7 GPa, which also did not deviate much from values reported in literature (14.8 GPa[35] and 15.8 GPa[32]), while the reported value by the manufacturer is 17.1 GPa. The E_f reported in literature for TET is 9.8 GPa[35], which is lower than what was obtained in this study (11.3±1.3 GPa), while no data available in literature for E_f of KAT. The E_f of ENA in literature ranges between

Table 5 Mean and standard deviation (between brackets) of the flexural load energy (U_r), and the intrablock homogeneity between the internal and external parts of each of the 10 blocks of the tested materials

Block	TET		KAT		CER		GRN		ENA	
	U_r (mJ)		U_r (mJ)		U_r (mJ)		U_r (mJ)		U_r (mJ)	
	Internal	External	Internal	External	Internal	External	Internal	External	Internal	External
1	20.8 (2.7)	21.9 (4.7)	44.5 (18.3)	45.3 (5.6)	35.2 (12.0)	39.9 (6.0)	19.1 (7.5)	21.1 (5.2)	2.5 (0.2)	2.4 (0.5)
2	39.6 (7.6)	33.3 (7.4)	30.6 (2.7)	27.8 (10.7)	38.1 (4.6)	37.1 (10.2)	23.7 (6.1)	20.2 (5.2)	2.6 (0.9)	2.8 (0.3)
3	35.5 (8.5)	37.3 (6.7)	29.1 (5.6)	32.7 (6.9)	28.0 (12.7)	38.7 (15.9)	22.5 (5.3)	22.7 (5.2)	2.7 (0.2)	2.6 (0.6)
4	26.4 (8.9)	30.1 (8.9)	39.1 (8.8)	37.6 (11.9)	30.0 (15.1)	32.8 (11.1)	19.2 (10.3)	24.7 (3.0)	3.0 (0.4)	3.3 (0.6)
5	25.1 (5.7)	22.7 (5.4)	34.0 (4.7)	33.4 (7.5)	31.9 (6.6)	30.9 (10.0)	25.9 (1.7)	26.4 (6.3)	2.7 (0.2)	2.7 (0.4)
6	24.5 (5.6)	26.2 (4.7)	39.7 (10.7)	43.5 (12.9)	24.2 (2.1)	29.6 (11.1)	29.3 (7.7)	24.2 (5.3)	3.2 (0.8)	3.5 (0.5)
7	22.6 (9.1)	23.3 (5.0)	35.2 (2.5)	43.8 (10.0)	33.8 (5.8)	28.6 (11.5)	21.1 (6.8)	22.2 (3.8)	3.1 (0.2)	2.7 (0.3)
8	36.0 (15.6)	29.3 (12.2)	36.5 (4.0)	41.7 (14.1)	16.3 (11.0)	24.6 (9.0)	24.6 (4.3)	23.4 (4.3)	3.6 (0.3)	3.2 (0.6)
9	20.8 (12.1)	27.8 (8.6)	29.9* (13.2)	48.1* (9.1)	20.8 (3.5)	25.6 (7.1)	23.4 (3.0)	23.7 (4.1)	2.2* (0.3)	2.8* (0.5)
10	38.7 (12.9)	37.3 (10.9)	33.4 (12.0)	40.4 (11.1)	18.3 (8.0)	25.5 (7.1)	24.8 (2.0)	22.8 (5.4)	3.2 (0.3)	3.4 (0.6)

* indicates a significant difference in homogeneity within the same block (Mann Whitney *U* test, $p<0.05$).

21.5–33.0 GPa[26-28,30,37-40], in comparison to 30.7±2.1 GPa in this study and 30.0±2 by the manufacturer.

Variations in results could be due to lack of standardization of the testing parameters among different laboratories, such as the number, size, storage or aging of samples, as well as the testing machines. Nevertheless, the inhomogeneity of CAD-CAM composite blocks, in particular, interblock inhomogeneity, should not be neglected.

Among the materials tested in this study, GRN has the highest σ_f significantly. This could be attributed to the reduced amount of flaws present, which could also be confirmed by its highest Weibull modulus reflected on its reliability. Although GRN has the highest wt% of fillers within the tested materials; yet, the correlation between σ_f and amount of fillers cannot be accurately deducted because the mass of fillers could vary leading to differences in vol%. Conversely, ENA had the highest E_f and HV significantly, despite having the lowest σ_f and U_r. Indeed, the microstructure of ENA is different, being formed from a pre-sintered ceramic network with large grain size that provides a rigid structure, thus having high E_f and HV[16]. At the same time, because less rigid materials can deform with shocks, E_f is inversely proportional to U_r, thus ENA and KAT have the lowest and highest U_r, respectively.

On the other hand, regarding flexural properties, intrablock inhomogeneity was observed between the external and internal parts of the tested materials GRN, CER, KAT and ENA, in which higher properties were shown at the external in comparison to the internal parts of the inhomogenous blocks (Tables 3–5). Interestingly, DF composites KAT, TET and GRN showed significantly higher HV internally than externally, ENA had higher HV externally, while CER was homogenous (Table 6 and Fig 3). This could be due to the different manufacturing process used for PICN (block infiltration) than for DF, but in the absence of information from manufacturers, this remains a hypothesis. Ilie[33] cut blocks into two and found, using indentation, higher E_f in the center than the periphery of the section, in GRN, as well as in TET. The suggested hypothesis was that since blocks are exposed to air during polymerization, this could lead to oxygen inhibition, which may create differences in the degrees of cross-linking[33]. However, a direct comparison with the present results is not possible because of the different methods used.

So far, to the authors' knowledge, no studies have

Table 6 Mean and standard deviation (between brackets) of the hardness (HV), and the intrablock homogeneity between the internal and external parts of each of the 10 blocks of the tested materials

Block	TET		KAT		CER		GRN		ENA	
	HV		HV		HV		HV		HV	
	Internal	External	Internal	External	Internal	External	Internal	External	Internal	External
1	76.0 (1.0)	75.3 (1.0)	74.1* (0.8)	69.2* (1.6)	87.7 (1.5)	87.5 (1.8)	121.8 (3.0)	122.5 (2.3)	214.2 (16.6)	223.3 (21.2)
2	77.9 (3.4)	74.3 (2.1)	73.7* (1.3)	69.8* (1.9)	90.0 (4.1)	87.7 (1.4)	124.0 (3.0)	124.0 (0.6)	208.7 (10.9)	215.7 (6.5)
3	74.7* (0.8)	73.3* (1.0)	67.9* (0.6)	73.3* (3.5)	85.7 (2.1)	84.4 (0.9)	125.7* (3.1)	129.3* (1.9)	210.3* (14.2)	233.5* (11.2)
4	73.8 (1.8)	72.1 (0.9)	69.3* (1.7)	72.3* (0.5)	83.1 (2.6)	84.3 (1.3)	121.0 (3.9)	122.5 (3.3)	221.5 (14.0)	214.7 (8.5)
5	74.3 (0.9)	73.5 (1.1)	73.9* (2.9)	69.8* (0.6)	87.6 (2.2)	88.9 (1.2)	130.7 (2.7)	129.2 (4.5)	214.0 (7.9)	232.0 (15.6)
6	74.9* (0.9)	73.4* (0.8)	72.8* (2.2)	68.7* (2.6)	84.8 (5.4)	91.8 (10.7)	124.3 (3.6)	126.7 (5.5)	225.7 (12.9)	232.3 (20.9)
7	74.8* (0.4)	73.6* (0.5)	74.7* (1.4)	66.4* (3.1)	87.0 (2.4)	84.3 (1.6)	126.3 (2.3)	127.8 (3.4)	224.2 (25.6)	236.5 (13.8)
8	73.8 (1.0)	73.3 (0.7)	73.6* (1.7)	68.7* (0.6)	84.6 (3.6)	85.5 (3.7)	126.7 (2.9)	122.2 (6.1)	214.5* (12.2)	233.2* (11.2)
9	72.2 (0.8)	72.6 (0.4)	71.1* (1.6)	67.4* (1.6)	87.4 (1.1)	86.1 (1.6)	129.0 (4.1)	126.3 (1.9)	217.0 (16.4)	223.2 (6.8)
10	73.3 (1.4)	74.3 (1.2)	72.3* (1.9)	66.5* (2.6)	91.4 (2.9)	89.2 (1.8)	129.2 (2.0)	127.5 (1.6)	211.8 (7.6)	226.5 (19.5)

* indicates a significant difference in homogeneity within the same block (Mann Whitney *U* test, $p<0.05$).

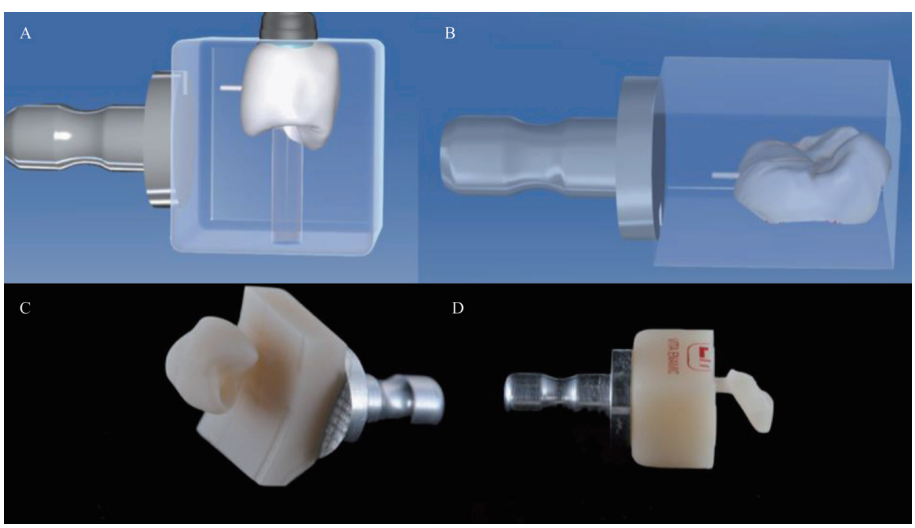

Fig. 6 Computer-aided design (CAD) and computer-aided manufacturing (CAM) of composite blocks. A and B, examples of CAD; C and D, examples of CAM. The position of the final restoration within the block is set up by the dental technician and can differ according to the restoration design. A thin restoration like a palatal veneer (Fig. 6D) or an occlusal table top does not need to be milled from the center of the block, which is weaker.

been found in literature on the interblock inhomogeneity of the mechanical properties between CAD-CAM composite blocks. This study highlights the different variations shown in all of the studied materials, which showed interblock inhomogeneity in one or more of the properties tested.

Different hypotheses could explain intrablock and interblock inhomogeneities encountered in the studied materials. Firstly, the mixing of monomers with fillers can lead to voids (Figs. 4, 5) and areas of inclusion (agglomerates of fillers not infiltrated by monomers) (Figs. 4A, 5B). Moreover, the filling process of the molds can also lead to the formation of air bubbles incorporated within the polymeric matrix, which were shown scattered all over the samples examined by digital and SEM (Figs. 4, 5). Furthermore, the HT polymerization process, which starts at the peripheries of the blocks and moves towards the center may result in internal stresses at the center of the block[33]. Additionally, the HT polymerization is accompanied by shrinkage of the matrix, and therefore should be compensated by HP[16].

Regarding the clinical implications of interblock inhomogeneity, it raises doubts concerning the reproducibility of the mechanical properties of CAD-CAM composite prostheses, which can vary with block selection and are, in general, lower than the values claimed by manufacturers.

Moreover, in this study, a small number of CAD-CAM composite blocks showed significant intrablock inhomogeneity in one or more of the mechanical properties tested (Tables 3–6 and Fig 3), which can further raise doubts regarding the homogeneity of the mechanical properties within a same prosthesis. Indeed, the procedure of fabrication of CAD-CAM restorations is a subtractive method, in which only part of the block is used for fabrication of the restoration, and the positioning of the prosthesis within the block, which is set up by the dental technician, can consequently influence the mechanical properties of the final restoration (Fig. 6). The present study highlights the fact that the internal or central parts can show lower mechanical properties than the external parts of CAD-CAM composite blocks (except for HV of DF it is the opposite) and therefore, suggests that restorations should not be positioned in the center of the block when possible.

CONCLUSION

Interblock and/or intrablock inhomogeneity of the mechanical properties was shown in all of the tested CAD-CAM composite materials. Dental practitioners and technicians should be aware of the possible interblock variations of CAD-CAM composites' mechanical properties while preparing prostheses and should not base their treatment approaches on manufacturers' data, which are often overoptimistic. Moreover, dental technicians should take intrablock variations into account when positioning the restoration within the block before milling, avoiding if possible, the center of the block. Finally, researchers should take into account inter- and intrablock variations when setting up protocols and interpreting the results of *in vitro* studies

ACKNOWLEDGMENTS

The authors thank Dr. Michael Sadoun for granting access of the equipment used in this study and his valuable scientific advices. Amélie Mainjot is married to the founder of the company MaJEB, which contributes to the development of PICN materials. The authors declare no other potential conflicts of interest with respect to the authorship and/or publication of this article. This research did not receive any specific grant from funding agencies in the public, commercial, or not-for-profit sectors.

REFERENCES

1) Coldea A, Fischer J, Swain MV, Thiel N. Damage tolerance of indirect restorative materials (including PICN) after simulated bur adjustments. Dental Mater 2015; 31: 684-694.
2) Lebon N, Tapie L, Vennat E, Mawussi B. Influence of CAD/CAM tool and material on tool wear and roughness of dental prostheses after milling. J Prosthet Dent 2015; 114: 236-247.
3) Chavali R, Nejat AH, Lawson NC. Machinability of CAD-CAM materials. J Prosthet Dent 2017; 118: 194-199.
4) Curran P, Cattani-Lorente M, Anselm Wiskott HW, Durual S, Scherrer SS. Grinding damage assessment for CAD-CAM restorative materials. Dent Mater 2017; 33: 294-308.
5) Pfeilschifter M, Preis V, Behr M, Rosentritt M. Edge strength of CAD/CAM materials. J Dent 2018; 74: 95-100.
6) Mainjot AKJ. The One step-No prep technique: A straightforward and minimally invasive approach for full-mouth rehabilitation of worn dentition using polymer-infiltrated ceramic network (PICN) CAD-CAM prostheses. J Esthet Restor Dent 2020; 32: 141-149.
7) Oudkerk J, Eldafrawy M, Bekaert S, Grenade C, Vanheusden A, Mainjot A. The one-step no-prep approach for full-mouth rehabilitation of worn dentition using PICN CAD-CAM restorations: 2-yr results of a prospective clinical study. J Dent 2020; 92: 103245.
8) Mainjot AK, Dupont NM, Oudkerk JC, Dewael TY, Sadoun MJ. From artisanal to CAD-CAM blocks: State of the art of indirect composites. J Dent Res 2016; 95: 487-495.
9) Zaghloul H, Elkassas DW, Haridy MF. Effect of incorporation of silane in the bonding agent on the repair potential of machinable esthetic blocks. Eur J Dent 2014; 8: 44-52.
10) Nguyen JF, Ruse D, Phan AC, Sadoun MJ. High-temperature-pressure polymerized resin-infiltrated ceramic networks. J Dent Res 2014; 93: 62-67.
11) Nguyen JF, Migonney V, Ruse ND, Sadoun M. Properties of experimental urethane dimethacrylate-based dental resin composite blocks obtained via thermo-polymerization under high pressure. Dent Mater 2013; 29: 535-541.
12) Phan AC, Béhin P, Stoclet G, Dorin Ruse N, Nguyen JF, Sadoun M. Optimum pressure for the high-pressure polymerization of urethane dimethacrylate. Dent Mater 2015; 31: 406-412.
13) Pomès B, Behin P, Jordan L, Legoff S, Stoclet G, Richaud E, *et al*. Influence of polymerization pressure and post-cure treatment on conversion degree and viscoelastic properties of polymer infiltrated ceramic network. J Mech Behav Biomed Mater 2021; 115: 104286.
14) Ribeiro BCI, Boaventura JMC, Brito-Gonçalves J de, Rastelli ANS, Bagnato VS, Saad JRC. Degree of conversion of nanofilled and microhybrid composite resins photo-activated by different generations of LEDs. J Appl Oral Sci 2012; 20:

212-217.
15) Leprince JG, Palin WM, Hadis MA, Devaux J, Leloup G. Progress in dimethacrylate-based dental composite technology and curing efficiency. Dent Mater 2013; 29: 139-156.
16) Nguyen JF, Migonney V, Ruse ND, Sadoun M. Resin composite blocks via high-pressure high-temperature polymerization. Dent Mater 2012; 28: 529-234.
17) Mörmann WH, Stawarczyk B, Ender A, Sener B, Attin T, Mehl A. Wear characteristics of current aesthetic dental restorative CAD/CAM materials: Two-body wear, gloss retention, roughness and Martens hardness. J Mech Behav Biomed Mater 2013; 20: 113-125.
18) Swain MV, Coldea A, Bilkhair A, Guess PC. Interpenetrating network ceramic-resin composite dental restorative materials. Dent Mater 2016; 32: 34-42.
19) Ludovichetti FS, Trindade FZ, Werner A, Kleverlaan CJ, Fonseca RG. Wear resistance and abrasiveness of CAD-CAM monolithic materials. J Prosthet Dent 2018; 120: 318.e1-318.e8.
20) Randolph LD, Palin WM, Bebelman S, Devaux J, Gallez B, Leloup G, *et al*. Ultra-fast light-curing resin composite with increased conversion and reduced monomer elution. Dent Mater 2014; 30: 594-604.
21) Ferracane JL. Elution of leachable components from composites. J Oral Rehabil 1994; 21: 441-452.
22) Krifka S, Spagnuolo G, Schmalz G, Schweikl H. A review of adaptive mechanisms in cell responses towards oxidative stress caused by dental resin monomers. Biomaterials 2013; 34: 4555-4563.
23) Giordano R. Materials for chairside CAD/CAM–produced restorations. J Am Dent Assoc 2006; 137: 14S-21S.
24) Koenig A, Schmidtke J, Schmohl L, Schneider-Feyrer S, Rosentritt M, Hoelzig H, *et al*. Characterisation of the filler fraction in CAD/CAM resin-based composites. Materials (Basel) 2021; 14: 1986.
25) Wendler M, Belli R, Petschelt A, Mevec D, Harrer W, Lube T, *et al*. Chairside CAD/CAM materials. Part 2: Flexural strength testing. Dent Mater 2017; 33: 99-109.
26) Awada A, Nathanson D. Mechanical properties of resin-ceramic CAD/CAM restorative materials. J Prosthet Dent 2015; 114: 587-593.
27) Lawson NC, Bansal R, Burgess JO. Wear, strength, modulus and hardness of CAD/CAM restorative materials. Dent Mater 2016; 32: e275-283.
28) Goujat A, Abouelleil H, Colon P, Jeannin C, Pradelle N, Seux D, *et al*. Mechanical properties and internal fit of 4 CAD-CAM block materials. J Prosthet Dent 2018; 119: 384-389.
29) Hampe R, Lümkemann N, Sener B, Stawarczyk B. The effect of artificial aging on Martens hardness and indentation modulus of different dental CAD/CAM restorative materials. J Mech Behav Biomed Mater 2018; 86: 191-198.
30) Lucsanszky IJR, Ruse ND. Fracture toughness, flexural strength, and flexural modulus of new CAD/CAM resin composite blocks. J Prosthodont 2020; 29: 34-41.
31) Grzebieluch W, Mikulewicz M, Kaczmarek U. Resin composite materials for chairside CAD/CAM restorations: A comparison of selected mechanical properties. J Healthc Eng 2021; 2021: 8828954.
32) Ling L, Ma Y, Malyala R. A novel CAD/CAM resin composite block with high mechanical properties. Dent Mater 2021; 37: 1150-1155.
33) Ilie N. Spatial distribution of the micro-mechanical properties in high-translucent CAD/CAM resin-composite blocks. Materials (Basel) 2020; 13: 3352.
34) International Organization for Standardization. ISO-6872: 2015. Dentistry—ceramic materials. Geneva: ISO; 2015.
35) Ducke VM, Ilie N. Aging behavior of high-translucent CAD/CAM resin-based composite blocks. J Mech Behav Biomed Mater 2021; 115: 104269.
36) Vichi A, Goracci C, Carrabba M, Tozzi G, Louca C. Flexural resistance of CAD-CAM blocks. Part 3: Polymer-based restorative materials for permanent restorations. Am J Dent 2020; 33: 243-247.
37) Lauvahutanon S, Takahashi H, Shiozawa M, Iwasaki N, Asakawa Y, Oki M, *et al*. Mechanical properties of composite resin blocks for CAD/CAM. Dent Mater J 2014; 33: 705-710.
38) Egilmez F, Ergun G, Cekic-Nagas I, Vallittu PK, Lassila LVJ. Does artificial aging affect mechanical properties of CAD/CAM composite materials. J Prosthodont Res 2018; 62: 65-74.
39) Yin R, Kim YK, Jang YS, Lee JJ, Lee MH, Bae TS. Comparative evaluation of the mechanical properties of CAD/CAM dental blocks. Odontology 2019; 107: 360-367.
40) Castro EF de, Azevedo VLB, Nima G, Andrade OS de, Dias CTDS, Giannini M. Adhesion, mechanical properties, and microstructure of resin-matrix CAD-CAM ceramics. J Adhes Dent 2020; 22: 421-431.